

Representation of the Denmark Strait Overflow in a z-coordinate eddy configuration of the NEMO (v3.6) ocean model: Resolution and parameter impacts” by Pedro Colombo et al.

Response to the Reviewer 1

We greatly appreciate comments which helped to largely improve the clarity of our manuscript. In the following, we provide our responses in a point-by-point manner. In our responses below, we use the following legend:

- *Italic characters* for the Reviewers’ comments.
- *Blue color* for our answers to the comments.
- *Blue color in italic* for the revised text, the specific changes being sometimes outlined in *magenta*.

Introduction

Reviewer's comment.

2-7 High salinity shelf water which is a source for Antarctic Bottom Water is an overflow too and could/should be mentioned here. Around Antarctica most models struggle to get the dense water from the shelf into the abyssal ocean without entraining too much surrounding water.

We agree, and we include explicitly this important process in the revised paper (Page 2, starting line 6). Note that this paragraph has also been modified to respond to the comments of reviewer 3.

“Overflows of important magnitude (not mentioning those crossing deep ocean ridges) are those associated with; the Denmark Strait and the Faroe Bank Channel where dense waters formed in the Arctic and the Nordic Seas flows into the North Atlantic (Girton and Standford, 2003, Brearley et al., 2012, Hansen and Østerhus, 2007); the strait of Gibraltar where dense and saline waters generated in the Mediterranean Sea overflow into the Atlantic Ocean (Baringer and Price, 1997); the strait of Bab-el-Manded where the highly saline Red Sea waters flow into the Gulf of Aden and the Indian ocean (Peters et al., 2005), and the continental shelves of the polar oceans (Killworth, 1977, Baines and Condie, 1998), in particular around Antarctica where the high salinity shelf waters formed in Polynyas ventilate the Antarctic Bottom waters (Mathiot et al., , Purkey et al., 2018). More reference papers can be found in Legg et al. (2009), Magaldi et al. (2015), Mastropole et al. (2017).”

We added two references.

Mathiot, P., Jourdain, N.C., Barnier, B., Gallée, H., Molines, J.-M., Le Sommer, J., and Penduff, T., 2012: Sensitivity of coastal polynyas and high-salinity shelf water production in the Ross Sea, Antarctica, to the atmospheric forcing. *Ocean Dynamics* 62, 701–723 (2012). <https://doi.org/10.1007/s10236-012-0531-y>.

Purkey S.G., Smethie W. M. Jr., Gebbie, G., Gordon, A. L., Sonnerup, R. E., Warner M. J., and Bullister, J. L., 2018: A Synoptic View of the Ventilation and Circulation of Antarctic Bottom Water from Chlorofluorocarbons and Natural Tracers. *Annu. Rev. Mar. Sci.*, 10:8.1–8.25. <https://doi.org/10.1146/annurev-marine-121916-063414>.

Methods

Reviewer's comment.

Figure 1. As far as I can tell, only section 29, 24, 20, 16 and Denmark Strait have been used. I do not see much value showing all the other sections. I suggest reducing them to the once which are being shown. I am aware that they are meant to show DSOW core.

Yes, the other sections are used in the study to calculate the path of the overflow. The integral calculations described in Appendix B are performed over the extent of these sections, integration across the section leading to the red spots which identify the path of the DSO in the control simulation.

We modified Fig. 1 which now includes only the 4 most relevant sections (see below).

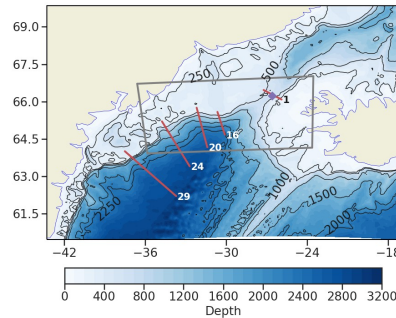
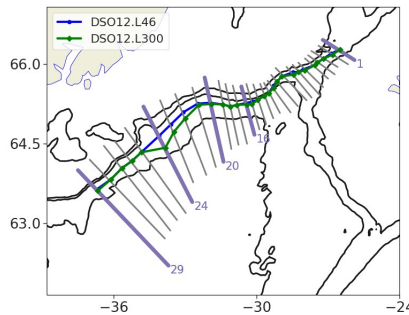


Figure 1. Regional model domain. In color the ocean depth. The 250, 500, 1000, 1500 and 2000 meter depth isobaths are contoured in black. The grey box indicates the region where the 2-way grid refinement ($1/36^\circ$ and $1/60^\circ$) is applied in some simulations. The location of the various sections used to monitor the model solution are shown by the red lines, and the numbered black lines for the most relevant ones. Section 1 is the reference section chosen for the sill. The thick dotted points indicate the center of the vein of the DSO in the Control simulation as calculated with the formulas given in Appendix B. The green dot indicates the reference point at the sill in order to calculate distances in Fig. 17.

The other sections are shown in the Appendix B (Fig. B1) where the calculation of the path of the overflow is discussed. The path of the overflow is also shown for the Control and the $1/60^\circ$ -150 Levels simulations in Fig. B1 (see below).

Figure and text in the Appendix B:



“Figure B1. Overflow path. Contours show the 500, 1000 and 2000 meter depth isobaths. The location of the various sections used to monitor the model solution are indicated by grey and purple lines. The blue/green dots indicate for each section the location of the center of the vein of the DSO in the Control simulation (blue, DSO12.L46) and in the $1/12^\circ$ 300 levels simulation (green, DSO12.L300), the blue/green lines outlining the path of the overflow in these simulations.”

The text below has been added in the Appendix B (Page 30).

“The position of the center of the overflow has been calculated with equations B1 and B2 at each of the 29 sections shown in Figure B1, thus defining the mean path of the overflow in the simulations. This path is used to produce the results shown in Fig. 9 and in Fig.17.”

Reviewer's comment.

Please see my comment how alternatively the DSOW could be tracked, which would not require individual sections.

Regarding the suggestion of an alternative way to track the DSOW with the minimum bottom temperature, it should work to define the path, but it may also face limitations especially in case of large salinity biases.

Because our sensitivity tests are scanning a large range of parameters, we cannot exclude cases where the bottom temperature signature of the overflow may hardly be different (or even warmer) from that of the ambient fluid, in case for example, of entrainment of highly saline waters. We expect difficulties with such method in simulations where the DSO is considerably unrealistic, which may happen when scanning a large set of parameters and resolutions. Our method based on the calculation of the center of mass and speed of the vein of fluid (Appendix B), which uses potential density and velocity, has the advantage to account for possible compensation in T/S biases and to provide, in addition to the location of the path, the depth of the core (not necessarily at the bottom) from which we can also approximate the thickness of the plume.

We decided to keep our method to calculate the path of the overflow (although we do not use the depth of the plume in the paper).

Reviewer's comment:

Figure 2. It is hard to compare those fields. I would suggest showing the mean from the global configuration and anomalies to the regional setup. In this case it becomes clearer where the differences are. Since both models use the same grid calculating anomalies should be easy.

We followed this recommendation and plotted the difference in current speed between global and control in subplots 2(c,d) instead of the current speed of Control, but the vectors are the currents of the Control. The vector field in these subplots is still the one from Control. We modified the figure legend and the text of the paper accordingly. At the moment the figures are built from the various subplots by Latex. We shall reduce spaces between subplots, as suggested in the next comment, in the final version of the paper.

The new figure legend is as follows:

“Figure 2. Surface (a) and bottom (b) mean currents (year 76) in the global ORCA12 simulation. Vectors/Colors indicate current direction/speed in $m.s^{-1}$. Surface (c) and bottom (d) mean currents (year 76) in the regional DSO12.L46 regional simulation. Vectors indicate direction and amplitude of the current. Colors indicate the current speed difference between the global and the regional simulation (in $m.s^{-1}$). Blue/red indicate that the current speed is greater/smaller in the Control (regional) simulation. Vectors at the bottom circulation are scaled by a factor of 7 compared to the surface for visibility reasons.”

Change in the text (Page 8, starting line 2).

“The large-scale circulation patterns is found to be very similar in both simulations, as illustrated with the surface and bottom currents shown in Fig. 2. The predominant currents such as the East Greenland Current (EGC), the Irminger Current (IC) and the DSO itself are very similar between the global and the regional model. This circulation scheme also compares well with that described from observations in Danialt et al. (2016) and from an ORCA12 model circulation simulation in Marzocchi et al. (2015).”

Reviewer's comment:

All the subsequent figures have a lot of white spaces between the subplots. If there is any chance to move subplot labels into the figures that would allow to reduce the white spaces and improve the visibility/readability of the figures.

We agree, and all figures will be modified in a way similar to that applied to Figure 2 before the revised paper is submitted.

Reviewer's comment:

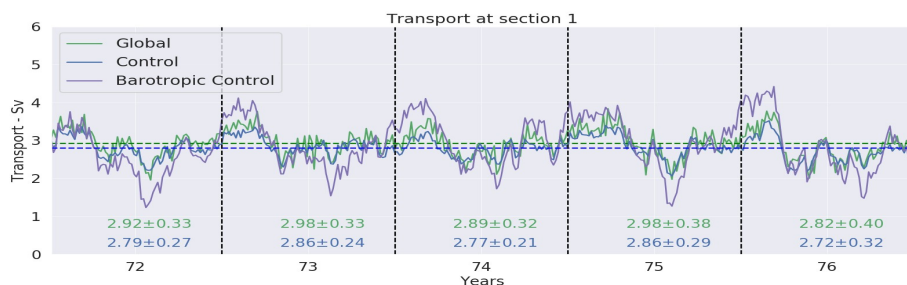
8-14. It appears that the DSOW has a seasonal cycle, which is not present in observations in the Denmark Strait (Jochumsen et al. 2012). Although this is not too critical for this study it shows that likely the formation regions of DSOW in the Nordic Seas are not captured correctly (Våge et al. 2013). That could explain why the transport variability is so low. The seasonal signal usually originates from the EGC and Fram Strait.

We agree that the seasonal cycle is not realistic and we now mention this in the revised paper (see below). What is important in this figure is that it demonstrates that the regional model is a reliable simulator of what the global model produces in that region, and therefore it is a “good result” that it reproduces this seasonal signal. The reviewer's remark led us to give a greater attention to this signal. Our investigation performed with the regional

model, revealed that it is the barotropic circulation that is driving this seasonal signal (see the new Figure 3). We address this issue by showing and discussing the barotropic transport in Figure 3.

The low values of the transport std shown in Fig. 3 are also a consequence of the sampling used for the model outputs which are 5-day means (the standard output of the global model simulations). Although the regional model outputs are daily means, we used 5-day means in this figure for the purpose of comparison with the global model. When daily means are used the std increases up to 0.7 Sv (more than double), but still remains below what is observed. We do not comment this in the paper, but we indicate in the figure legend that

Modified Figure 3:



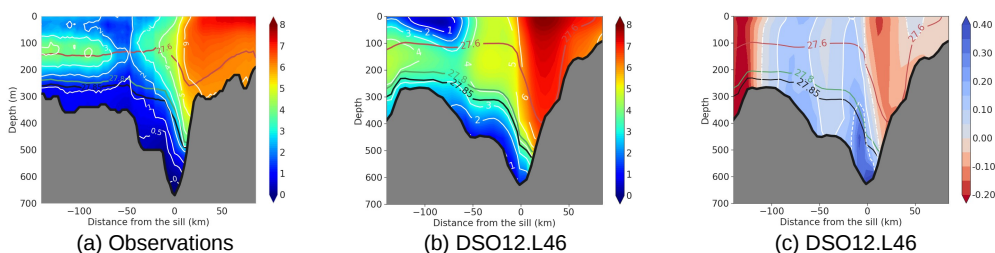
“Figure 3. Time evolution of the volume transport of waters of potential density greater than 27.80 kgm^{-3} at the sill section (Section 1 in Fig. 1) in the Control (blue line) and the Global (green line) simulations (the latter providing the open boundary conditions). Annual mean and std (in Sv) are indicated for every individual year of simulation. The depth-integrated (barotropic) transport is shown for the Control simulation (purple line). 5-day mean values are used to produce this figure.”

Modified text (page 8, line 16):

“The standard deviation computed from 5-day outputs ($\sim 0.3 \text{ Sv}$ in the control run, increasing to 0.7 Sv when calculated from daily values) is rather small when compared to the 1.6 Sv of Macrander et al. (2005). The modelled flow of dense waters presents a marked seasonal cycle which is not present in observations (Jochumsen et al. 2012). This signal is the signature of the large seasonality of the barotropic flow (Fig. 3) that constrains the whole water column.”

Figure 4. I would swop (a) and (b) so you can avoid starting in line 8-16 with Figure 4b and later going back to Figure 4a.

This figure has been modified to include a plot showing the observations of Mastropole et al. (2017). The Figure legend and the text have been modified as follows in the revised version of the paper.



“Figure 4. Mean flow characteristics (annual mean of year 76) in the global simulation at the sill. Temperature ($^{\circ}\text{C}$) in colours and white contours for (a) the observations (Mastropole et al., 2017) and (b) the control simulation ($1/12^{\circ}$ and 46 vertical levels). Potential density values (σ_{θ}) are shown by the contour lines coloured in red (27:6), green (27:8) and black (27:85). (c) The velocity normal to the section in the control simulation (southward velocity in blue colour being negative). White lines indicate the 0 ms^{-1} contour (dotted line), the -0.1 ms^{-1} (full line) and the -0.2 ms^{-1} contour (dashed line). The model section being taken along the model coordinate, the topography is slightly different in the model.”

The text now reads:

“Fig. 4 presents the characteristics of the mean flow across the sill. The model simulation is compared to the data of Mastropole et al. (2017) who processed over 110 shipboard hydrographic sections across Denmark Strait (representing over 1000 temperature and salinity profiles) to estimate the mean conditions of the flow at the sill. Compared with the compilation of observations of Mastropole et al. (2017) (Fig. 4a) the model simulation (Fig. 4b) shows a similar distribution of the isopycnals, specially the location of the 27.8 isopycnal. However, the observations exhibit waters denser than 28.0 in the deepest part of the sill which the model does not reproduce. Large flaws are noticed regarding the temperature of the deepest waters which are barely below 1°C when observations clearly show temperatures below 0°C (also seen in the observations presented in e.g. Jochumsen et al. (2012), Jochumsen et al. (2015), Zhurbas et al. (2016)). A bias toward greater salinity values (not shown) is also found in the control experiment which shows bottom salinity of 34.91 compared to 34.9 in the observations shown in Mastropole et al. (2017), but the resulting stratification in density shows patterns that are consistent with observations. The distribution of velocities (Fig. 4c) is also found realistic when compared with observations (i.e. the Fig. 2b of Jochumsen et al. (2012)) with a bottom intensified flow of dense waters (up to 0.4 ms⁻¹) in the deepest part of the sill. Although the present setup is designed to investigate model sensitivity in twin experiments and not for comparison with observations ends, the control run appears to provide a flow of dense waters at the sill that is stable over the 5 year period of integration and reproduces qualitatively the major patterns of the overflow “source waters” seen in the observations. Therefore, despite existing biases, the presence of a well identified dense overflow at the sill confirms the adequacy of the configuration for the sensitivity studies.”

Figure 5-6 (Fig. 6-7 in the revised paper). Is there the chance to include observational values here (CTD casts) along some of these sections? That would help to illustrate how the solution should look like.

As we say in the paper (section 2.2), the initial conditions of the simulations, which come from a long term (~90 years) global simulation, are significantly different from observations, as the flaws in the representation of the overflows (and other flaws) have modified the mass field (too warm and salty, as discussed). The main objectives of these figures is to compare the solution in twin sensitivity experiments.

To address this comment, we decided to add one figure (Figure 5 in the revised paper, see below), comparing the model solution to observations at a given section. This figure compares the model with observations collected during the ASOF project (Quadfasel, 2004) at the downstream-most section among those shown in the paper (i.e. section 29 in Fig. 1). We chose that section because it is a good illustration of the major flaws of the “end product” in the Control run (the plume is too warm, diluted, does not reach deep enough, and is hardly distinguishable from the ambient fluid). It complements Fig. 4 which shows the “source waters”. It also provides guidance regarding assessment of improvements which will be acknowledged if the plume is colder, or deeper, or separated from the ambient fluid by sharper gradients. We modified the text of the paper accordingly. New Figure 5:

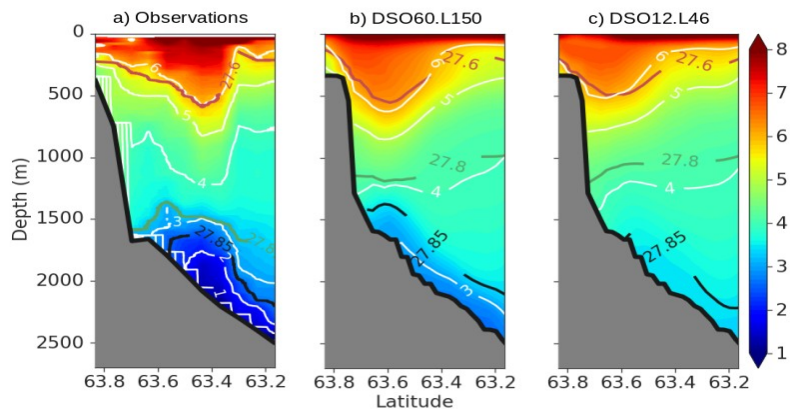


Figure 5: Potential Temperature (°C) at section 29 in (a) the observations (ASOF6-section, Quadfasel, 2004), (b) the 1/60°, 150 levels simulation (annual mean), and (c) the 1/12°, 46 level simulation (annual mean). Red/Green/Black full lines are isopycnals 27.6/27.8/27.85. White lines are isotherms by 1°C interval. For Fig.

b), the section 29 is outside (~100 km downstream) the 1/60° AGRIF zoom, so the effective resolution is 1/12°. But the water masses acquired their properties upstream within the 1/60° resolution zoom. Observation data were downloaded at: <https://doi.pangaea.de/10.1594/PANGAEA.890362>.

Text changes related to this Fig.5 (page 8, starting line 31):

“Finally, in order to assess improvements in the sensitivity tests, the major flaws of the control simulation must be described. If similarities with observations are found at the sill, the evolution of the DSO plume in the Irminger basin is shown to be unrealistic in the present setup of the control simulation, and presents the same flaws as in the global run. This is demonstrated by the analysis of the temperature and potential density profiles at the most downstream cross-section (section 29) where the model solution is compared to observations (Fig. 5), and at the other cross-sections along the path of the DSO in the Control simulation (the plots on the left hand side of Fig. 6 and 7). The evolution of the DSO plume as it flows southward along the East Greenland shelf break is represented by a well-marked bottom boundary current (e.g. the bottom currents in Fig. 2) carrying waters of greater density than the ambient waters. Far downstream the sill (section 29) the observations show a well-defined plume of cold water confined below the 27.8 isopycnal under 1500 m depth (Fig. 5a). The bottom temperature is still below 1°C. In the Control simulation (Fig. 5c), one can clearly identify the core of the DSO plume by the 27.85 isopycnal, so it is clear that the plume has been sinking to greater depth as it moved southward. This evolution is only qualitatively consistent with the observations at this section. The modelled plume is significantly warmer and exhibits a core temperature of 3.5° (against 2°C or less in the observations). The plume is also much wider than observed, exhibits much smaller temperature and salinity gradients separating the plume from the interior ocean, indicating a greater dilution with ambient waters. The plume is barely distinguishable from the ambient fluid below 2000m when it is still well marked at that depth in the observations. The sinking and dilution of the plume as it flows southward along the slope of the Greenland shelf is well illustrated in Fig. 6 and 7 (left hand panels) which display the potential temperature at the other sections. If the overflow waters are still well-marked at section 16 (Fig. 6a), it is barely distinguishable from the ambient water at section 29.”

Maybe just adding density contours would/could already help.

Main isopycnals (27.6, 27.8 and 27.85) are present in every plot showing vertical sections.

9-1 *It remains unclear where this statement is based on, as far as I can tell observations along these sections are not shown or provided.*

This statement is based on the comparison with the ASOF sections shown in Quadfasel (2004). This remark suggests that this is not clearly formulated. We consider that the addition of the new Figure 5 and the changes in the text to account for it are clarifying this issue.

Reviewer's comment:

I recommend a re-write of section 8-29 until the results section. The main point is not clear to me. Is it that in the control simulation the temperature in the DSOW layer are more diluted than in the other simulation? If so, this should go in the results section and would also help avoid talking about Figure 7 twice.

Section 2.3 has three parts that each have a specific purpose to set the paradigm of our study that is: what we shall learn from the regional model will be relevant for the global model, the model solution with the “standard” (i.e. used in most global simulations) parameterization and resolution produces a well-identified overflow so the regional model is relevant for this study, and major flaws in the representation of the overflow properties are identified so it will be possible to assess improvements.

The first part (Page 7 starting line 5) demonstrates that the Regional model reproduces faithfully the global model solution. It ends with: *“Therefore this regional model appears as a reliable simulator of what the global model produces in that region”*. This part is essential part of the paradigm of the study.

The second part (Page 8 starting line 10) describes the properties of the source waters (at the sill) and characterizes their flaws. This part is important because a reasonable degree of realism is needed at the sill for the study of the DSO. This part has been improved by adding in Fig. 4 the observations by Mastropole et al. (2017). This part ends with the following statement: *“Therefore, despite existing biases, the presence of a well*

identified dense overflow at the sill confirms the adequacy of the configuration for the sensitivity studies". It has been slightly modified to account for the additional plot showing observations.

The third part (Page 8 starting line 29) characterizes, in the control simulation, the flaws in the representation of the overflow along its path, i.e. at the 4 downstream sections for which there are observations from Quadfasel (2004). The main point of this section is to characterize the major flaws of the control experiment, and to demonstrate that they are not different from the flaws of the global model.

The reviewer's comment indicates that its objective of the third part was not made very clear in the text. We consider that the addition of the new Fig. 5 and the changes in the text relative to this part (see our comments about Fig. 5 above) are clarifying this issue especially since we introduce more clearly the objective, this part beginning with (Page 8 starting line 31):

"Finally, in order to assess improvements in the sensitivity tests, the major flaws of the control simulation must be qualified."

Results:

Figure 7 (Fig. 8 in the revised paper). Is it necessary to show the "warm" $>3.6^\circ\text{C}$ waters? It distracts from the cold DSOW in the Irminger Sea and would allow to get a bit more structure in these plots. Have you tried using anomalies plots here, to make the point clear that with more vertical levels the bottom water gets eroded?

Interesting comment. We modified the plots using a color palette that emphasizes waters below 4°C . Indeed we found that this change makes the figure more readable.

Reviewer's comment:

Figure 7,10,11 (8,11,12 in the revised paper). I think it would help to overlay the DSOW path in these simulations.

We did not overlay the DSO path on these figures because it tends to mask the details of the overflow properties, especially in their initial descent. We show the overflow path for two of our simulations in Fig. B1 in the Appendix and the reader can refer to this figure. The overflow path, as calculated in Appendix B, is used to make Figures 9.

Fig. 1B and the associated text have been shown above is the discussion of Fig. 1.

Reviewer's comment:

As the authors stated the DSOW is characterized by a temperature minimum, so the path in these simulations could be also defined by the zonal minimum in the regional for each latitude, an alternative way to what the authors use at present.

Regarding the calculation of the path of the overflow, we already answered this comment before, and we decided to keep our method to calculate the path of the overflow.

Reviewer's comment:

22-14 I am not convinced that reducing the model bias in the source waters will help. Results in Figure 16 (Fig. 17 in the revised paper) show that even if modelled temperature would agree with observations, temperatures downstream would end up being warmer than the observations.

We agree with the referee's analysis of Fig. 16 (Fig. 17 in the revised version). Nevertheless, there is no chance to obtain a realistic representation of the DSO if the source waters (i.e. the waters at the sill and the ambient waters) do not have the correct properties. Therefore, reducing the bias in the sources waters is a necessary condition, but will likely not be sufficient. We slightly modified the text to make this clearer (page 23 line 26):

"Improved initial and boundary conditions (i.e. correcting for the warm bias of 0.3°C at the sill and for the warm and salty bias of the entrained waters of the Irminger Current) should reduce this difference, but to a point which is difficult to estimate. Either way, the 1.5°C difference shown in Fig. 17 is a quite wide gap that such bias correction will likely not be sufficient to fill."

Technical corrections:

I could not spot any typos but hope a native speaker might help.

We did our best with our co-authors.